Critical step length as an indicator of surface supersaturation during crystal growth from solution

Robert Darkins,[†] Ian J. McPherson,[‡] Ian J. Ford,[†] Dorothy M. Duffy,[†] and Patrick R. Unwin*,[‡] †London Centre for Nanotechnology, University College London, 17-19 Gordon Street, London, WC1H 0AH, UK

‡Department of Chemistry, University of Warwick, Coventry, CV4 7AL, UK
Received October 27, 2021; E-mail: p.r.unwin@warwick.ac.uk

Abstract: The surface processes that control crystal growth from solution can be probed in real-time by in situ microscopy. However, when mass transport (partly) limits growth, the interfacial solution conditions are difficult to determine, precluding quantitative measurement. Here, we demonstrate the use of a thermodynamic feature of crystal surfaces—the critical step length—to convey the local supersaturation, allowing the surface-controlled kinetics to be obtained. Applying this method to atomic force microscopy measurements of calcite, which are shown to fall within the regime of mixed surface/transport control, unites calcite step velocities with the Kossel-Stranski model, resolves disparities between growth rates measured under different mass transport conditions, and reveals why the Gibbs-Thomson effect in calcite departs from classical theory. Our approach expands the scope of in situ microscopy by decoupling quantitative measurement from the influence of mass transport.

The surface of a crystal growing from solution can be inspected by in situ microscopy to determine the rates and mechanisms of growth, 1-4 as well as the kinetic and thermodynamic effects of additives. 5-8 These experimental techniques advance our basic understanding of crystallisation and inform our efforts to control it, e.g. in the pursuit of new nanomaterials⁹ and growth inhibitors. ¹⁰ However, in situ measurements are difficult to interpret when the solution conditions at the surface of the crystal are unknown. This situation can arise when a crystal depletes the surrounding solutes to produce a concentration gradient with a surface supersaturation that deviates from the bulk value. Under this regime of mixed surface/transport control, the surface processes become sensitive to variables that influence mass transport. For example, the distribution, and therefore the history, of steps across the crystal surface will affect the rate of solute depletion; confinement 11 and probe geometry 12 can impact convective transport; impurities can yield kinetic effects with non-monotonic flow rate dependencies; 13 and mixed control coupled with stochastic step production can drive kinetic instabilities. 14 Complicated processes may therefore conceal the surface supersaturation.

In this work, we identify the critical step length (defined below) as a readily measurable surface feature that can immediately reveal the interfacial solution conditions by functioning as a yardstick for the local supersaturation. We demonstrate how this feature can be used to recover the true surface-controlled kinetics of a growing crystal by analysing atomic force microscopy (AFM) data for calcite (CaCO₃) published across a series of seminal papers. ^{1–3} These particular data were chosen because they include the most com-

prehensive set of critical length measurements available, but also because of the broad importance of calcium carbonate, both in the real world and as a rich model system. While the significance of mass transport is well-established in the context of calcite dissolution, ¹⁵ its importance to calcite growth has hitherto been downplayed by the crystal growth community. It will be shown that flow-through AFM studies of calcite growth are significantly limited by mass transport, and that accounting for this effect can bridge the gap between experimental observation and basic models of crystal growth.

In situ AFM is usually performed within a fluid cell where a flowing solution replenishes the solutes consumed by the growing crystal. Increasing the flow rate diminishes the concentration boundary layer until the reaction becomes limited by the surface kinetics. In practice, this state of surface control is purportedly achieved once the step velocities have lost their flow rate dependence. ¹⁶ However, owing to the complex hydrodynamics of experimental systems, flow rate dependencies can become too weak to be resolved even far from conditions of surface control. 17-19 We have demonstrated this with a finite element analysis of the AFM apparatus in refs., $^{1-3}$ where solutes were transported by convection and diffusion through a fluid cell containing a growing crystal of calcite and a probe (Fig. 1a). Flux boundary conditions at the crystal surface approximated the experimental crystal growth rates, and the degree of mass transport to a microscopic scan area on the crystal surface was characterised by a boundary layer thickness δ as a function of the flow rate $u \ (\delta \approx 418u^{-0.27} \ \mu \text{m} \text{ where } u \text{ is in mL/hr, Fig. 1b}).$ In the AFM experiments, the step velocities were reported to exhibit flow rate independence across $30 \lesssim u \lesssim 40 \text{ mL/hr.}^{16}$ For comparison, the surface supersaturation in the model changed by 3% across this flow range, which is too small to be resolved by AFM measurements of the step velocity, and yet the surface supersaturation deviated substantially from the bulk (Fig. 1a).

The true supersaturation at the crystal surface in the AFM experiments can be revealed by examining the surface thermodynamics. A step segment on the surface of a crystal is propelled forward by a chemical potential driving force, where each new ionic row reduces the free energy by an amount proportional to the step length. Resisting this step advance is the free energy cost of extending the length of the two orthogonally adjacent steps. It follows that a finite critical step length L_c exists at which these competing effects balance and the step velocity vanishes,

$$L_c = \frac{2a\phi}{k_B T \ln S_{\text{surf}}} \tag{1}$$

where a = 0.32 nm is the lattice spacing of a single ion

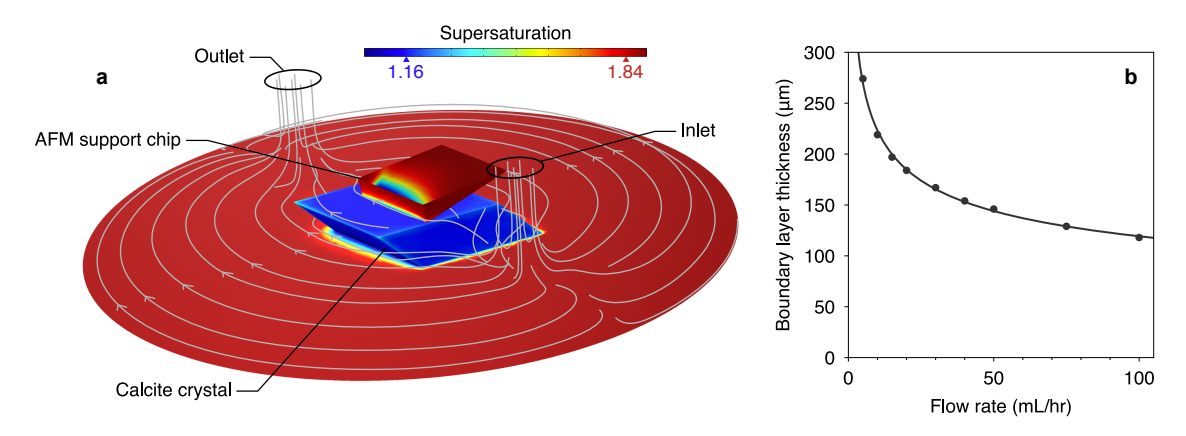


Figure 1. Finite element model of an AFM fluid cell. (a) A rhombohedral calcite crystal (2 mm in width), AFM support chip, and the base of a fluid cell are shown. The colours represent the supersaturation across the surfaces, and the streamlines show the passage of flow between the inlet and outlet. The flow rate is 30 mL/hr. (b) The dependence of boundary layer thickness on solution flow rate in the finite element model, evaluated in a region of the crystal surface under the AFM tip (circles). The line is a power law fit.

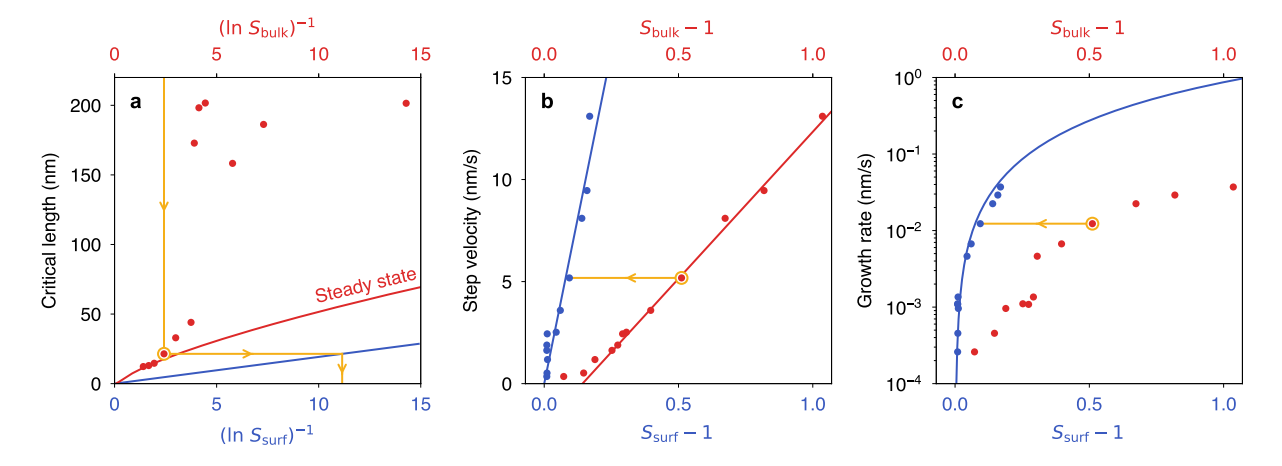


Figure 2. AFM calcite kinetics recalibrated against the surface supersaturation. (a) The theoretical relationship between L_c and S_{surf} (equation (1)) is shown by the blue line. AFM-derived measurements of L_c (red circles) are larger, reflecting the differences between S_{bulk} and S_{surf} . The measurements are consistent with a steady state correlation (red line) after substantial surface reconstruction, achieved in this case only for large supersaturations. (b) The obtuse step velocities from AFM (red circles) recalibrated against S_{surf} (blue circles). The lines are drawn to guide the eye. See the Supporting Information for the acute step velocities. (c) The normal growth rate (red circles) recalibrated against S_{surf} (blue circles). The line is a theoretical fit. (a-c) All AFM measurements (circles) have been reproduced from ref. ² The yellow arrows depict, for a single datum, the procedure of using L_c to map from S_{bulk} to S_{surf} .

in calcite, ϕ is the average step free energy per ion, k_B is Boltzmann's constant, T is the temperature, and $S_{\rm surf}$ is the supersaturation at the surface of the crystal. We distinguish $S_{\rm surf}$ from the bulk value $S_{\rm bulk} = \sqrt{a_{\rm Ca}a_{\rm CO_3}/K_{\rm sp}}$, where $a_{\rm Ca}$ and $a_{\rm CO_3}$ are the ion activities in bulk solution and $K_{\rm sp}$ is the solubility product of calcite. In crystals that exhibit crystallographically nonequivalent step types, such as the acute and obtuse steps of calcite, each step type will have a distinct stability, and this stability will be reflected in the thermodynamic driving force for growth that underpins L_c . In particular, equation (1) will correspond to the critical length of the least stable step type—the obtuse step in the case of calcite. This perspective of nonequivalent step types conflicts with previous accounts, and we explain it in the Supporting Information.

Critical lengths are manifested at screw dislocations and in the two-dimensional nucleation of islands. 1,20,21 For calcite, L_c has been directly measured by observing the motion of nascent step segments nucleated at screw dislocations. ¹ However, we focus here on ref., ² where the critical lengths were not directly measured, but where they can be inferred

geometrically from the reported step velocities and terrace widths (circles in Fig. 2a). For calcite grown under surface control ($S_{\rm surf} = S_{\rm bulk}$), the critical lengths should follow the blue line in Fig. 2(a), which is a plot of equation (1) with a step free energy $\phi = 3k_BT$. ²² However, the experimental results are an order of magnitude too large. This discrepancy between experiment and theory, which has been noted previously, ²³ indicates that the supersaturation at the surface must have been substantially lower than in the bulk, in agreement with our finite element analysis.

Once the role of mass transport is recognised, the experimental dependence of L_c on $S_{\rm bulk}$ becomes straightforward to interpret. When a crystal is first exposed to a fresh solution, its surface will reconstruct in response. However, it takes time for the new step trains to spread from the dislocation sources across the surface. If sufficient time is allowed for large-scale reconstruction, then L_c will converge to a steady state curve with a dependence on $(\ln S_{\rm bulk})^{-1}$ that is nonlinear due to the feedback loop between surface structure and $S_{\rm surf}$ (red line in Fig. 2a); if only partial reconstruction is achieved, then L_c will depend on the stochastic

history of the surface (see the low supersaturation points in Fig. 2a); and if negligible reconstruction occurs across a series of distinct solution conditions, then L_c will display a linear dependence on $(\ln S_{\rm bulk})^{-1}$, but the function will be notably offset from the origin such that L_c extrapolates to zero at $(\ln S_{\rm bulk})^{-1} \approx \frac{1}{2}$ (precisely as observed in the direct measurements of L_c^{-1}). See the Supporting Information for a mathematical treatment of these cases.

Irrespective of the surface structure, even far from steady state, the critical length only depends on the prevailing surface supersaturation, and so $S_{\rm surf}$ can always be computed from the measured critical length using equation (1). The true saturation state associated with any measurement x, such as a step velocity, may also be recovered from L_c as long as the locales of x and L_c are similar enough to experience an identical solution environment (we estimate that points within $\sim 10~\mu{\rm m}$ can be assumed to share a solution environment for AFM studies of calcite). In other words, L_c allows a nominal measurement $(S_{\rm bulk}, x)$ to be decoupled from solute transport and mapped to its surface-controlled analogue $(S_{\rm surf}, x)$. Applying this technique to the kinetic data from ref. immediately solves two fundamental problems in calcite kinetics.

First, basic growth theory contends that the step velocities of a Kossel crystal should scale as $\sim (S_{\rm surf}-1)$ at low supersaturation, owing to the statistical independence of attachment and detachment events. This contrasts with the observations of ref. which exhibit a non-linear dependence on $S_{\rm bulk}$, with a linear segment that is offset from the saturation point (red circles in Fig. 2b). These non-linearities, discussed further in ref., have motivated investigations into non-Kossel kinetic models. However, recognising that $S_{\rm surf}$ and $S_{\rm bulk}$ are different due to mixed surface/transport control, the step velocities can be recalibrated as a function of $S_{\rm surf}$, revealing a linear dependence consistent with the Kossel-Stranski model (blue circles in Fig. 2b).

Second, a recent microfluidic study 25 measured the normal growth rate of calcite to be two orders of magnitude faster than AFM 2 under nominally similar conditions. The authors speculated that mass transport may have limited growth in the AFM experiments. Indeed, using the critical length to recalibrate the growth rates against $S_{\rm surf}$ yields surface-controlled rates that are two orders of magnitude faster (Fig. 2c), bringing the AFM and microfluidic measurements to within a factor of ~ 4 .

Mixed surface/transport control can also have subtle kinetic consequences. The dependence of step velocity v(L) on the step segment length L remains an outstanding problem in basic growth theory.²⁶ In extreme cases of mass transport control, as well as for high kink density crystals, the step velocity satisfies the length-dependence $v(L)/v(\infty) =$ $S_{\rm bulk} - S_{\rm bulk}^{L_c/L}$, which we shall refer to as the Gibbs-Thomson rule. ²⁰ This rule is widely applied, often beyond the conditions for which it was derived. However, highly polygonal crystals with an inter-kink spacing comparable to the thermodynamic critical length may fail to satisfy the fluctuationdissipation theorem, resulting in a critical length much larger than the thermodynamic prediction and, significantly, a step velocity that rises abruptly beyond this kinetically determined critical length. 27 Calcite has been likened to these extremely low kink density crystals, with the suggestion that it too fails to implement the fluctuation-dissipation theorem. 26,28 However, we have already shown that the unexpectedly large critical lengths of calcite can be attributed to

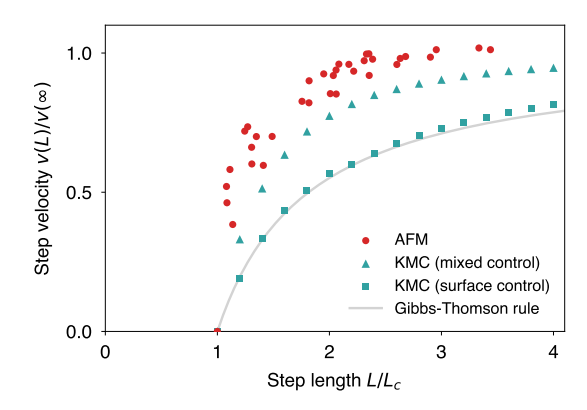


Figure 3. Step velocity dependence on step length. The AFM measurements were taken from ref. 1 and span 1.19 $\leq S_{\rm bulk} \leq 1.51$. KMC simulations that are representative of surface-controlled growth $(S_{\rm surf} = S_{\rm bulk} = 1.51)$ are consistent with the Gibbs-Thomson rule, which deviates significantly from AFM. By contrast, KMC simulations that are representative of mixed kinetic control $(S_{\rm surf} = 1.043,$ derived from the critical length corresponding to the $S_{\rm bulk} = 1.51$ AFM measurement) is more consistent with the AFM velocity profile.

mixed surface/transport control, and we argue that its step velocity profile v(L) can be similarly ascribed. Using kinetic Monte Carlo (KMC) simulation, we have computed v(L) for a calcite-like Kossel crystal for cases representative of surface control ($S_{\rm surf} = S_{\rm bulk}$) and mixed surface/transport control ($S_{\rm surf} \ll S_{\rm bulk}$). The case of surface control was consistent with the Gibbs-Thomson rule, while mixed control was consistent with AFM to within a trivial normalisation error (Fig. 3). For calcite, the rapid rise in velocity with step length is therefore a consequence of the low surface supersaturation (large critical length) that characterises mixed control.

In conclusion, if the conditions at a crystal/solution interface are unknown, then the information provided by in situ microscopy is, at best, underutilised. At worst, the observations can be misinterpreted if surface control is wrongly assumed, e.g. based on the weak dependence of mass transport on flow rate, as we have demonstrated for AFM studies of calcite. In particular, the effects of mass transport can be mistaken for non-Kossel kinetics or a failure of thermodynamics. However, when the critical step length can be established, the transport effects—including the complexities of surface history—can be straightforwardly accommodated. For this reason, we advocate that future in situ studies of crystal growth under mixed surface/transport control be accompanied by sufficient data to recover the corresponding critical lengths. In some crystal systems, the critical length would first need to be characterised before our technique could be applied. It is encouraging that many further problems in the field of crystal growth theory may be readily solved upon correcting for mass transport in this way. For example, the dependence of calcite kinetics on solution stoichiometry has proven difficult to reconcile with theory. $^{29,30}\,$ Significantly, the existing analysis has neglected mass transport, and so this problem is a candidate for a similar treat-

Supporting Information Details of the finite element model, the theoretical analysis of AFM kinetics, and the KMC simulations are available online.

Acknowledgments This work was supported by an Engineering and Physical Sciences Research Council (EPSRC) Programme Grant (EP/R018820/1).

References

- Teng, H. H.; Dove, P. M.; Orme, C. A.; De Yoreo, J. J. Thermodynamics of calcite growth: baseline for understanding biomineral formation. Science 1998, 282, 724-727, DOI: 10.1126/science.282.5389.724.
- Teng, H. H.; Dove, P. M.; De Yoreo, J. J. Kinetics of calcite growth: surface processes and relationships to macroscopic rate laws. Geochimica et Cosmochimica Acta 2000, 64, 2255-2266, DOI: 10.1016/S0016-7037(00)00341-0.
- Teng, H. H.; Dove, P. M.; DeYoreo, J. J. Reversed calcite morphologies induced by microscopic growth kinetics: insight into biomineralization. Geochimica et Cosmochimica Acta 1999, 63, 2507-2512, DOI: 10.1016/S0016-7037(99)00103-9.
- (4) Dove, P. M.; Hochella Jr, M. F. Calcite precipitation mechanisms and inhibition by orthophosphate: In situ observations by scanning force microscopy. Geochimica et Cosmochimica Acta $\textbf{1993},\ 57,\ 705-714,\ \mathrm{DOI}\colon 10.1016/0016-7037(93)90381-6.$
- Shtukenberg, A. G.; Ward, M. D.; Kahr, B. Crystal growth with macromolecular additives. *Chemical reviews* **2017**, *117*, 14042– 14090, DOI: 10.1021/acs.chemrev.7b00285.
- (6) Fu, G.; Qiu, S. R.; Orme, C. A.; Morse, D. E. De Yoreo, J. J. Acceleration of calcite kinetics by abalone Morse, D. E.: nacre proteins. Advanced Materials 2005, 17, 2678-2683, DOI: 10.1002/adma.200500633.
- (7) Elhadj, S.; De Yoreo, J. J.; Hoyer, J. R.; Dove, P. M. Role of molecular charge and hydrophilicity in regulating the kinetics of
- molecular charge and hydrophilicity in regulating the kinetics of crystal growth. Proceedings of the National Academy of Sciences 2006, 103, 19237–19242, DOI: 10.1073/pnas.0605748103. Wasylenki, L. E.; Dove, P. M.; Wilson, D. S.; De Yoreo, J. J. Nanoscale effects of strontium on calcite growth: An in situ AFM study in the absence of vital effects. Geochimica et Cosmochimica Acta 2005, 69, 3017–3027, DOI: 10.1016/j.gca.2004.12.019.

 Meldrum, F. C.; Cölfen, H. Controlling mineral morphologies
- and structures in biological and synthetic systems. Che Reviews 2008, 108, 4332-4432, DOI: 10.1021/cr8002856.
- (10) Ma, W.; Lutsko, J. F.; Rimer, J. D.; Vekilov, P. G. Antagonistic cooperativity between crystal growth modifiers. Nature 2020, *577*, 497–501, DOI: 10.1038/s41586-019-1918-4.
- (11) Maeki, M.; Yamazaki, S.; Takeda, R.; Ishida, A.; Tani, H.; Tokeshi, M. Real-time measurement of protein crystal growth rates within the microfluidic device to understand the microspace effect. ACS Omega 2020, 5, 17199–17206, DOI: 10.1021/acsomega.0c01285.
- (12) Burt, D. P.; Wilson, N. R.; Janus, U.; Macpherson, J. V.; Unwin, P. R. In-situ atomic force microscopy (AFM) imaging: influence of AFM probe geometry on diffusion to microscopic surfaces. *Langmuir* **2008**, *24*, 12867–12876, DOI: 10.1021/la8003323.
- (13) Maruyama, M.; Kawahara, H.; Sazaki, G.; Maki, S.; Takahashi, Y.; Yoshikawa, H. Y.; Sugiyama, S.; Adachi, H.; Takano, K.; Matsumura, H.; Inoue, T.; Murakami, S.; Mori, Y. Effects of a forced solution flow on the step advancement on {110} faces of tetragonal lysozyme crystals: direct visualization of individual steps under a forced solution flow. Crystal Growth
 \(\begin{align*} \text{B Design 2012, 12, 2856-2863, DOI: 10.1021/cg300025b. } \)
 (14) Vekilov, P. G.; Rosenberger, F. Increased stability in crys-
- tal growth kinetics in response to bulk transport enhancement. *Physical Review Letters* **1998**, 80, 2654, DOI: 10.1103/PhysRevLett.80.2654.
 Agrawal, P.; Bollermann, T.; Raoof, A.; Iliev, O.; Fischer, C.; Wolthers, M. The contribution of hydrodynamic processes to
- calcite dissolution rates and rate spectra. Geochimica et Cos-
- mochimica Acta 2021, DOI: 10.1016/j.gca.2021.05.003.

 (16) Fan, C.; Chen, J.; Chen, Y.; Ji, J.; Teng, H. H. Relationship between solubility and solubility product: The roles of crystal sizes and crystallographic directions. Geochimica et Cosmochimica Acta 2006, 70, 3820-3829, DOI: 10.1016/j.gca.2006.06.011.
- Gasperino, D.; Yeckel, A.; Olmsted, B. K.; Ward, M. D.; Derby, J. J. Mass transfer limitations at crystallizing interfaces in an atomic force microscopy fluid cell: A finite element analysis. *Langmuir* **2006**, *22*, 6578–6586, DOI: 10.1021/la060592k.
- (18) Peruffo, M.; Mbogoro, M. M.; Adobes-Vidal, M.; Unwin, P. R. Importance of mass transport and spatially heterogeneous flux processes for in situ atomic force microscopy measurements of crystal growth and dissolution kinetics. *The Journal of Physical Chemistry C* **2016**, *120*, 12100–12112, DOI:
- 10.1021/acs.jpcc.6b03560. (19) Adobes-Vidal, M.; Shtukenberg, A. G.; Ward, M. D.; Unwin, P. R. Multiscale visualization and quantitative analysis of L-cystine crystal dissolution. Crystal Growth & Design 2017, 17, 1766-1774, DOI: 10.1021/acs.cgd.6b01760.
- Burton, W. K.; Cabrera, N.; Frank, F. C. The growth of crystals and the equilibrium structure of their surfaces. *Philosoph*ical Transactions of the Royal Society of London. Series Mathematical and Physical Sciences 1951, 243, 299–358, DOI: 10.1098/rsta.1951.0006.

- (21) Malkin, A. J.; Land, T. A.; Kuznetsov, Y. G.; McPherson, A.; DeYoreo, J. J. Investigation of virus crystal growth mechanisms by in situ atomic force microscopy. Physical Review Letters 1995, 75, 2778, DOI: 10.1103/PhysRevLett.75.2778.
- Söhnel, O.; Mullin, J. W. Precipitation of calcium carbonate. *Journal of Crystal Growth* **1982**, *60*, 239–250, DOI: 10.1016/0022-0248(82)90095-1.
- Chernov, A. A.; Rashkovich, L. N.; Vekilov, P. G. Steps in solution growth: dynamics of kinks, bunching and turbulence. *Journal of Crystal Growth* **2005**, *275*, 1–18, DOI:
- 10.1016/j.jcrysgro.2004.10.094. Chernov, A. A.; Rashkovich, L. N.; DeYoreo, J. J. ABC of kink kinetics and density in a complex solution. AIP Conference Pro-
- ceedings. 2007; pp 34-47, DOI: 10.1063/1.2751908.

 (25) Li, L.; Sanchez, J. R.; Kohler, F.; Røyne, A.; Dysthe, D. K. Microfluidic control of nucleation and growth of CaCO3. Crystal Growth & Design 2018, 18, 4528–4535, DOI: 10.1021/acs.cgd.8b00508.
- Chernov, A. A. Notes on interface growth kinetics 50 years after Burton, Cabrera and Frank. *Journal of Crystal Growth* **2004**, 264, 499-518, DOI: 10.1016/j.jcrysgro.2003.12.076.
- (27) Rashkovich, L. N.; Gvozdev, N. V.; SilâĂŹnikova, M. I.; Yamin-skii, I. V.; Chernov, A. A. Dependence of the step velocity on its length on the (010) face of the orthorhombic lysozyme crystal. Crystallography Reports 2001, 46, 860-863, DOI: 10.1134/1.1405879.
- De Yoreo, J. J.; Zepeda-Ruiz, L. A.; Friddle, R. W.; Qiu, S. R.; Wasylenki, L. E.; Chernov, A. A.; Gilmer, G. H.; Dove, P. M. Rethinking classical crystal growth models through molecular scale insights: consequences of kink-limited kinetics. Crystal Growth & Design 2009, 9, 5135-5144, DOI: 10.1021/cg900543g.
- (29) Sand, K. K.; Tobler, D. J.; Dobberschütz, S.; Larsen, K. K.; Makovicky, E.; Andersson, M. P.; Wolthers, M.; Stipp, S. L. S. Calcite growth kinetics: dependence on saturation index, $Ca^{2+}: CO_3^{2-}$ activity ratio, and surface atomic structure. Crystal Growth & Design **2016**, 16, 3602–3612, DOI: 10.1021/acs.cgd.5b01792.
- Andersson, M. P.; Dobberschütz, S.; Sand, K. K.; Tobler, D. J.; De Yoreo, J. J.; Stipp, S. L. S. A microkinetic model of calcite step growth. *Angewandte Chemie* **2016**, *128*, 11252–11256, DOI: 10.1002/ange.201604357.